PHYSICAL REVIEW B

CONDENSED MATTER

THIRD SERIES, VOLUME 25, NUMBER 2 15 JANUARY 1982

Dynamics of silver ions in the superionic conductor Ag_3SI

P. Brüesch, H.U. Beyeler, and S. Strässler
Brown Boveri Research Center, CH-5405 Baden, Switzerland
(Received 17 August 1981)

The far-infrared reflectivity $R(\tilde{\omega})$ of β-Ag_3SI and γ-Ag_3SI has been measured in the range $5<\tilde{\omega}<400$ cm^{-1} and at various temperatures between 90 and 300 K. The most interesting feature is the observation of a resonance near $\tilde{\omega}_0=60$ cm^{-1} and a pronounced increase of $R(\tilde{\omega})$ below 40 cm^{-1}; the latter disappears below $T_c=157$ K, the $\beta\rightarrow\gamma$ phase-transition temperature. These data can be interpreted successfully on the basis of a microscopic model in which the silver ions move in a double-well potential. The oscillation of the silver ions in the wells gives rise to the resonance near $\tilde{\omega}_0=60$ cm^{-1} while the jumps across the potential barrier lead to the observed increase of $R(\tilde{\omega})$ below 40 cm^{-1}. The height of the potential barrier is between 250 and 400 K. The interpretation of our optical data is supported by recent structural investigations.

I. INTRODUCTION

Ag_3SI belongs to the large family of Ag-based superionic conductors such as AgI, Ag_2S, $RbAg_4I_5$, $(C_5H_5NH)Ag_5I_6$, $AgCrS_2$, etc. The crystal structure as well as the transport and thermal properties of this compound have been studied in detail.[1-7] It is now well established that Ag_3SI possesses three crystallographic phases. In α-Ag_3SI the anions, I and S, are distributed statistically over the centers and the corners of the cubic unit cell, while the silver ions are distributed over a large number of available sites located on the faces of the cube, a distribution which is similar to the one in α-AgI [Fig. 1(a)]. α-Ag_3SI is a mixed conductor with a dominating and very large ionic conductivity of about 1 $(\Omega\,\text{cm})^{-1}$ at 300°C.[2] The potential barriers for diffusion of silver ions are estimated to be 0.03—0.05 eV.[2,7] At 519 K a first-order phase transition to the β phase occurs in which the anions are ordered, but the silver ions are still disordered as shown in Fig. 1(b). As in α-Ag_3SI there are still four possible sites for silver ions on each cube face, but these sites are now much closer to the face centers, the distance from the centers being only 0.5 Å (the corresponding distance in α-Ag_3SI is $a/4=1.248$ Å). This structure leads to basically two kinds of jumps for the silver ions:

(1) local jumps between the four equivalent sites grouped around a face center, and

(2) diffusive jumps of a silver ion from one face of the cube to a neighboring face [Fig. 1(b)].

The potential barrier for the diffusive jumps is relatively high, of the order of 0.17 eV as estimated from the ionic conductivity which is about 0.02 $(\Omega\,\text{cm})^{-1}$ at 300 K.[2] On the other hand, the potential barrier for the local jumps is much lower; a value of only 0.014 eV has been estimated on the basis of recent x-ray data.[6] Finally, at 157 K there is a phase transition into the γ phase; this phase transition is very close to second order.[3] γ-Ag_3SI is an ordered structure which is closely related to the structure of β-Ag_3SI. The positions of the anions are almost the same as in βAg_3SI, while Ag is located at one of the four positions of the β phase obeying a threefold symmetry axis around the [111] axis [Fig. 1(c)]. Accordingly, the structure is no longer cubic but belongs to the rhombohedral system. Figure 1 also displays schematically the expected behavior of the mean potential energy of silver ions in the three phases.

In this paper we are studying the dynamical behavior of the silver ions in Ag_3SI by means of far-infrared optical studies. Since the dielectric response of α-Ag_3SI will be complicated by the nonvanishing electronic conductivity we are focusing our attention on the β and γ phases. The β

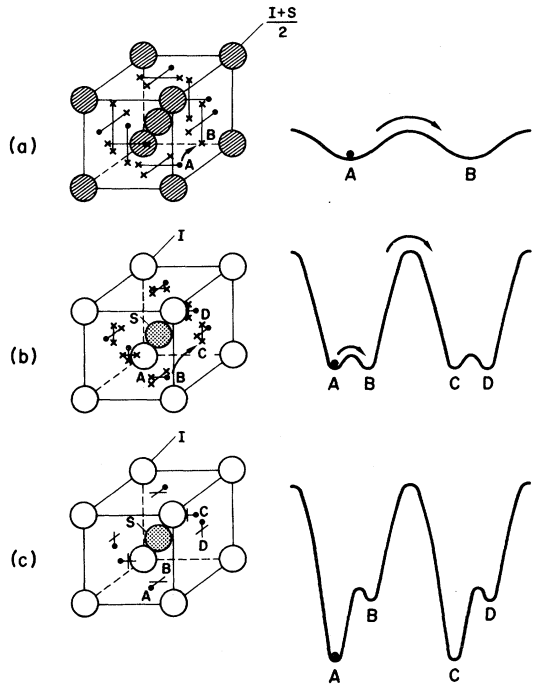

FIG. 1. (a) Structure of α-Ag_3SI and schematic potential energy for the motion of silver ions. (b) Structure of β-Ag_3SI and schematic potential energy for silver ions (local jumps $A \leftrightarrow B$ across double-well potential, diffusive jumps $B \rightarrow C$ across large potential barriers). (c) Structure of γ-Ag_3SI; the silver ions are locked in the deep potential wells A and C.

phase is clearly of great interest due to the possibility of the silver ions of rattling between the four equivalent sites grouped around each face center. In a linear model and disregarding the diffusive jumps across the large potential wells we can consider the motion of the silver ions to be that in a symmetric double-well potential.

In Sec. II we present our reflectivity measurements of β- and γ-Ag_3SI in the far infrared. In β-Ag_3SI we observe a characteristic increase of the reflectivity below about 40 cm^{-1}; this low-frequency structure completely disappears in the γ phase. In Sec. III we interpret and discuss the experimental data on the basis of ions moving in a symmetric double-well potential and show that the increase of the reflectivity is due to jumps of silver ions across the small energy barrier of the double-well potential.

II. EXPERIMENTAL

Crystals of Ag_3SI were grown by the Bridgman technique. Stoichiometric amounts of Ag_2S and AgI were sealed into a quartz ampoule, melted, and then slowly pulled through a temperature gradient centered around 700°C. Ingots were polycrystals containing large single-crystal domains which were used for the reflectivity measurements.

All far-infrared measurements have been performed with a Beckman FS 720 interferometer. For measurements above 150 cm^{-1} the instrument was used in the Michelson mode and below 150 cm^{-1} in the polarizing mode.[8] The measurements have been performed with a dc mercury source. Both a Golay cell and germanium bolometer operated at 1.5 K have been used as a detector. Most spectra have been recorded with a resolution of 1.2 cm^{-1}. A specially constructed reflection cell has been used the details of which are described elsewhere.[9] The samples were cooled with a central stream of cold nitrogen gas while the windows (sealed with normal O rings) were kept near room temperature by a peripheral hot stream of nitrogen. This guarantees a uniform temperature over the whole sample. In order to avoid the disturbing reflectivity from the windows, the cell is equipped with oblique windows. The sample holder carrying the sample and the reference mirror was rotatable.

Figure 2 shows the reflectivity of β-Ag_3SI at 300 K and of γ-Ag_3SI at 90 K between 10 and 360 cm^{-1}. At room temperature we observe two broad absorptions near 200 and 250 cm^{-1} and a rather well-defined reflectivity peak near 60 cm^{-1}. Note the pronounced increase in the reflectivity R below 40 cm^{-1}.

At 90 K the peaks are considerably sharper and shifted towards higher frequencies. In addition, weak subsidiary structures appear, for instance, near 30 and 70 cm^{-1}; they probably arise from the lowering of the symmetry in going from the β into the γ phase. Note that at 90 K the reflectivity is essentially flat at low frequencies. Figure 3

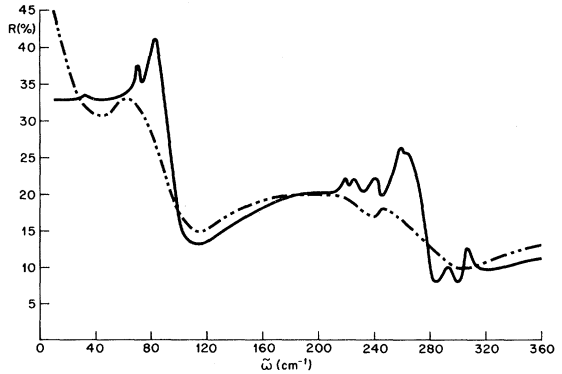

FIG. 2. Reflectivity of β-Ag_3SI at 300 K (— ·· — ·· —) and of γ-Ag_3SI at 90 K (——).

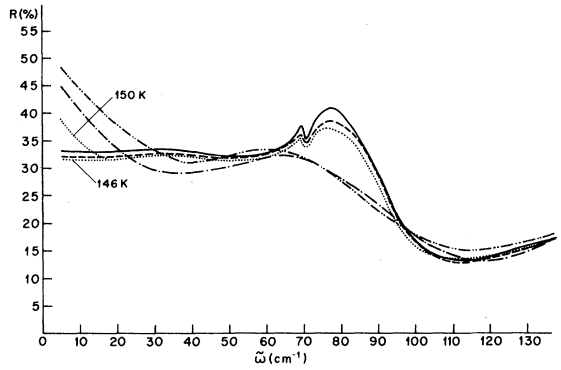

FIG. 3. Temperature dependence of the reflectivity of β-Ag_3SI and γ-Ag_3SI. $T=300$ K (— ·· — ·· —); $T=180$ K (— · — · —); $T=146$ and 150 K (· · ·); $T=134$ K (— — —); $T=90$ K (——). The $\beta\rightarrow\gamma$ phase transition temperature is at 156 K. The small increase of the reflectivity below 20 cm^{-1} at 150 K is regarded as a precurser effect of the phase transition.

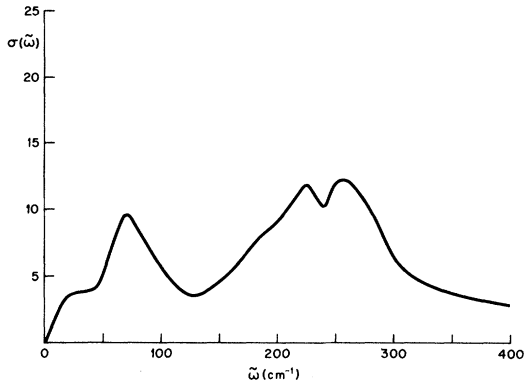

FIG. 5. Frequency-dependent conductivity $\sigma(\tilde{\omega})$ as obtained from a Kramers-Kronig analysis of the reflectivity of β-Ag_3SI at 300 K; below 5 cm^{-1} the reflectivity has been extrapolated with the help of the double-well model. The shoulder below 40 cm^{1} is due to the jumps of the silver ions across the double-well potentials.

displays the temperature dependence of the reflectivity between 5 and 140 cm^{-1}. The increase in R at low frequencies is observed at 300, 180, and 150 K. The $\beta\rightarrow\gamma$ phase transition is at 157 K. We regard the small increase in R at 150 K as a precurser effect of the phase transition. Below 146 K the reflectivity is flat down to 5 cm^{-1}, the low-frequency limit of our instrument.

The temperature dependence of the peak frequency of the low-frequency mode is shown in Fig. 4. With decreasing temperature there is a marked increase in the peak frequency in the vicinity of the $\beta\rightarrow\gamma$ phase transition at 157 K. Figure 5 displays the frequency-dependent conductivity $\sigma(\tilde{\omega})$ as obtained from a Kramers-Kronig analysis of the observed reflectivity at 300 K; below 5 cm^{-1} $R(\tilde{\omega})$ has been extrapolated using the double-well model discussed in Sec. III. Figure 6 shows $\sigma(\tilde{\omega})$ of γ-Ag_3SI at 90 K.

III. INTERPRETATION OF EXPERIMENTS AND DISCUSSION

Considering the structure of β-Ag_3SI [Fig. 1(b)] it is evident that the dynamics of the ions in this phase is very complicated. From a lattice dynamical point of view the unit cell contains five ions which are coupled by short- and long-range forces; furthermore, the silver ions are disordered and can jump between the four possible sites close to the face centers. A generalized lattice-dynamical model has been developed for simple diatomic

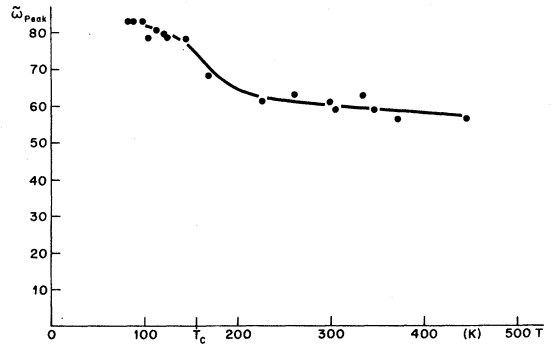

FIG. 4. Temperature dependence of the low-frequency optical mode near 60 cm^{-1}. Note the change in frequency near $T_c=156$ K.

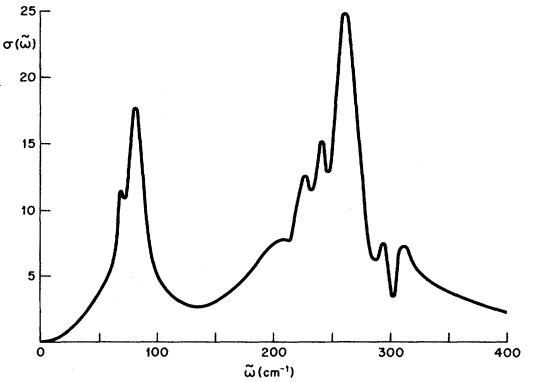

FIG. 6. Frequency-dependent conductivity $\sigma(\tilde{\omega})$ as obtained from a Kramers-Kronig analysis of the reflectivity of γ-Ag_3SI at 90 K.

crystals in which one sublattice of particles has two or more equivalent positions in a lattice site.[10–12] The application of such a model to β-Ag_3SI is, however, very involved as will be discussed at the end of this section.

We therefore adopt a different point of view, namely an Einstein-type model in which the direct coupling between the ions is neglected, and within this model we are focusing our attention to the local motion of one silver ion. The limitations of this model will be discussed below. If the silver ion is displaced perpendicularly to its cube face containing the four equivalent sites, it will move in a normal single-well potential [Fig. 1(b)]. We are not concerned with this motion but rather with the motion of the silver ion within its cube face. In an applied field this motion becomes essentially one dimensional, i.e., the motion in a double-well potential [Fig. 1(b)], and there are in a certain approximation two separate responses to an applied light field: (1) the vibration of the silver ion within one of the wells of the double-well potential which is represented by a damped oscillator leading to a resonance in the reflectivity near the oscillator frequency ω_0, and (2) the jump process described by a Debye relaxation leading to a structure near the Debye relaxation frequency. These two responses should qualitatively explain the behavior of the reflectivity of β-Ag_3SI below 150 cm^{-1} (Fig. 3).

The frequency-dependent mobility of a Brownian particle moving in a double-well potential has been studied by Schneider and Strässler.[13] The nonlinear equation of motion is

$$m\ddot{x} = -m\gamma\dot{x} - U'(x) + f(t), \tag{1}$$

where m is the mass of the particle, $-m\gamma\dot{x}$ is the damping force, $U'(x)$ is the derivative of the double-well potential $U(x) = \Delta(x^4 - 2x^2)$ with barrier height Δ, and $f(t)$ is a random force which describes the coupling of the particle with the thermal motion of the lattice. The latter is assumed to be Gaussian white noise with $\langle f(t)f(t')\rangle = 2\gamma m k_B T\delta(t-t')$ where T denotes the temperature and k_B Boltzmann's constant. Equation (1) has been solved by means of continued fraction approximations. These results are remarkably well reproduced by a simple memory function ansatz[13,14] which we use here for fitting the experimental data.

The reflectivity is given by

$$R = \left| \frac{\sqrt{\epsilon} - 1}{\sqrt{\epsilon} - 1} \right|^2, \tag{2}$$

where $\epsilon(\omega)$ is the complex dielectric constant. The relation between $\epsilon(\omega)$ and the frequency-dependent conductivity $\sigma(\omega)$ is

$$\epsilon(\omega) = \epsilon_\infty + 4\pi\frac{\sigma(\omega)}{-i\omega}. \tag{3}$$

Here, ϵ_∞ is the high-frequency dielectric constant. $\sigma(\omega)$ can be expressed in terms of the mobility $\mu(\omega)$ by

$$\sigma(\omega) = f\mu(\omega), \tag{4}$$

where f is the oscillator strength. The expression for $\mu(\omega)$ based on the memory function ansatz is given in the Appendix. The model contains five parameters, namely: the oscillator frequency ω_0, the oscillator strength f, the oscillator damping γ, the "high-frequency dielectric constant" ϵ_∞, and Δ/k_BT. Figure 7 shows fits of the model to the observed reflectivity of β-Ag_3SI at three different temperatures. In these fits the parameters ω_0, f, ϵ_∞, and Δ are almost the same, while γ decreases slightly with decreasing temperature. For the barrier height Δ we find 0.029 eV, corresponding to a temperature of 338 K. Figure 8 shows the real and the imaginary part of the dielectric constant as well as the ionic conductivity σ as a function of frequency, as obtained from the fit of the model to the reflectivity at 300 K. Within the Einstein-type model the main resonance in $\sigma(\tilde{\omega})$ near 75 cm^{-1} is due to the oscillation of the silver ion in the potential well, while the shoulder below about 30 cm^{-1} originates from the jumps of the silver ions across the potential barrier. The escape rate, defined as the probability per unit time for a silver ion to escape from a well over a barrier, is given by (see the Appendix)

$$1/\tau_{esc} = \omega_{esc} = 2\pi c\tilde{\omega}_{esc} = c\tilde{\omega}^* s e^{-\Delta/k_BT}. \tag{5}$$

Here $\tilde{\omega}^*$ is the renormalized oscillation frequency and s is a factor defined in the Appendix. $s\tilde{\omega}^*$ can be regarded as the attempt frequency in wave number for jumps. At 300 K we obtain $\tilde{\omega}^* = 77$ cm^{-1}, $s\tilde{\omega}^* = 70$ cm^{-1}, and $1/\tau_{esc} = 6.2 \times 10^{11}$ sec^{-1} corresponding to $\tilde{\omega}_{esc} = 3.3$ cm^{-1}. The low-frequency peak of $\epsilon_2(\tilde{\omega})$ is at $\tilde{\omega}_p = 2\tilde{\omega}_{esc} = 6.6$ cm^{-1} (Fig. 8).

The fits shown in Fig. 7 are based on trial and error. We have also performed least-square fits by varying all five parameters or only a smaller number of parameters and have obtained essentially the same parameters and quality of the fits as those of Fig. 7. It should be mentioned that the fit of the model to the observed reflectivity allows only an

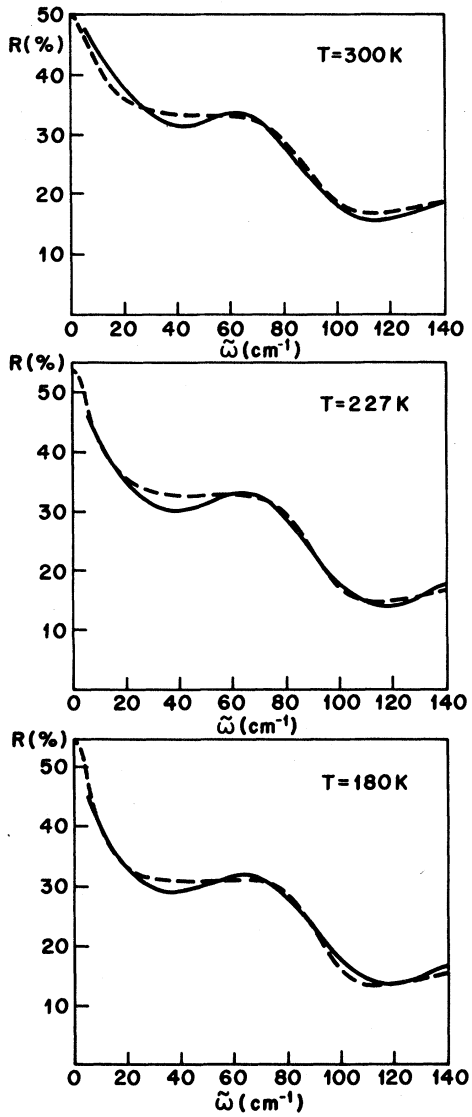

FIG. 7. Fits of the double-well model to the observed reflectivity of β-Ag_3SI at $T=300$, 227, and 180 K. ——: experimental; — — —: model fit. The parameters are $\tilde{\omega}_0=90$ cm^{-1}, $f=2200cm^{-2}$, $\tilde{\gamma}=25$ cm^{-1}, $4\Delta/k_BT=4.5$, $\epsilon_\infty=8$ at 300 K; $\tilde{\omega}_0=90$ cm^{-1}, $f=2200$ cm^{-2}, $\tilde{\gamma}=21$ cm^{-1}, $4\Delta/k_BT=6$, $\epsilon_\infty=7.5$ at 227 K; $\tilde{\omega}_0=90$ cm^{-1}, $f=2000$ cm^{-2}, $\tilde{\gamma}=19$ cm^{-1}, $4\Delta/k_BT=7.5$, $\epsilon_\infty=7$ at 180 K. The barrier height Δ is 0.029 eV which corresponds to 338 K.

approximate determination of the barrier height Δ: We have performed least-square fits with ω_0, f, γ, and ϵ_∞ as the variable parameters and with different fixed values of Δ. It is possible to obtain reasonable fits with values of Δ ranging between about 250 and 400 K; values of Δ outside this range gave definitely poorer fits, especially below 40 cm^{-1}. Thus we have shown that the microscopic double-well model with the expression (5) for the escape rate is able to describe qualitatively the experiments. The model describes both the oscillation (resonance near 75 cm^{-1}) and the jumps [shoulder of $\sigma(\tilde{\omega})$ below 30 cm^{-1}] of the silver ions and predicts a barrier height Δ between 250 and 400 K.

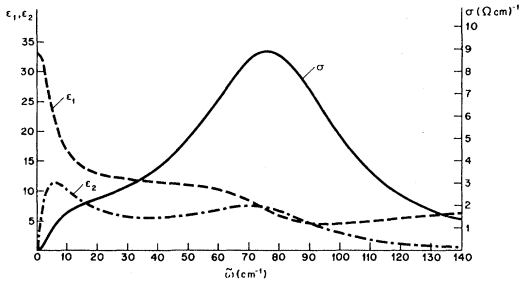

FIG. 8. Frequency dependence of the dielectric constant and ionic conductivity of β-Ag_3SI at 300 K as obtained from a fit of the double-well model to the observed reflectivity. $\epsilon_1(\tilde{\omega})$: — — —; $\epsilon_2(\tilde{\omega})$: —·—·—; $\sigma(\tilde{\omega})$: ——. The peak in $\epsilon_2(\tilde{\omega})$ at $\tilde{\omega}=6.6$ cm^{-1} and the shoulder in $\sigma(\tilde{\omega})$ below about 30 cm^{-1} are due to the jump of silver ions across the double-well potentials.

Above T_c the small barrier height Δ gives rise to a damping $1/\tau'$ (see the Appendix) in addition to the oscillator damping γ. At 180 K the values are $1/\tau'\cong 35$ cm^{-1} and $\tilde{\gamma}\cong 19$ cm^{-1}. Well below T_c the silver ions move in a single-well potential which means that the "additional damping" $1/\tau'$ disappears. At T_c the oscillator damping γ will also change due to the change in crystal structure which manifests itself in the appearance of new weak absorption peaks (Figs. 2, 3, and 6). Even if γ increases slightly at T_c, the net effect will result in a smaller damping below T_c leading to a considerably sharper resonance as observed in Figs. 3 and 6. The drop in the damping at T_c will renormalize the oscillator frequency towards higher values. This effect together with the slightly larger force constants explains the increase of the resonance frequency at T_c as observed in Fig. 4.

In the double-well model considered above the oscillatory motion and the jump motion are intimately coupled; the prefactor of the escape rate, $1/\tau_{esc}$ [Eq. (5)], is not an independent parameter but depends on ω_0, γ, and Δ (see the Appendix). This is one of the reasons that only fits of moderate quality are obtained (Fig. 7). For this reason we have considered in addition a phenomenological model in which the oscillation is completely decoupled from the jumps. The oscillatory

motion is described by a damped oscillator while the jumps are represented by a Debye relaxation process, thus

$$\epsilon(\omega)=\epsilon_\infty+\frac{4\pi B_D}{1-i\omega\tau_D}+\frac{4\pi f}{\omega_0^2-\omega^2-i\gamma\omega}. \quad (6)$$

This model contains six parameters, namely ϵ_∞, B_D, τ_D, f, ω_0, and γ. Figure 9 shows a least-square fit of this model to the reflectivity at 300 K. The fit is good below 100 cm^{-1} but less satisfactory above. For the Debye relaxation frequency $\omega_D = 1/\tau_D = 2\pi c\tilde{\omega}_D$ we find 14.6×10^{11} sec^{-1}, which corresponds to $\tilde{\omega}_D = 7.3$ cm^{-1}; this is the peak frequency of $\epsilon_2(\tilde{\omega})$ and is close to the corresponding value $2\tilde{\omega}_{esc} = 6.6$ cm^{-1} of the double-well model. Assuming that $\tilde{\omega}_D$ is thermally activated and choosing a barrier height $\Delta = 338$ K we obtain about the same attempt frequency as for the double-well model. The fact that the two models give approximately the same prefactor shows that the two degrees of freedom (oscillation and jumps) are related. If the degrees of freedom would be unrelated, the prefactors would, in general, be different. The microscopic double-well model is thus confirmed and provides a good description of the basic physics.

One should note that, from first principles, the independent-oscillator—Debye model is not consistent because the degrees of freedom representing the Debye mode are not an independent part of the lattice dynamics. In particular, the sum rule for $\sigma(\omega)$ (Ref. 15) is not satisfied by such a model. The advantage of the microscopic double-well model lies in the fact that a qualitative fit is possible with only five parameters and that it obeys the sum rule.

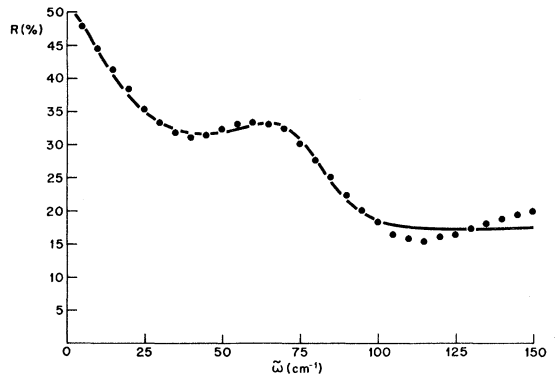

FIG. 9. Least-squares fit of the independent-oscillator—Debye-relaxation model according to Eq. (6) to the reflectivity of β-Ag_3SI at 300 K. The parameters are $\tilde{\omega}_0=71.3$ cm^{-1}, $f=983.9$ cm^{-2}, $\tilde{\gamma}=32.7$ cm^{-1}, $\epsilon_\infty=6.14$, $B_D=2.07$, $\tau_D^{-1}=14.6\times10^{11}$ sec^{-1}.

In applying the double-well model to Ag_3SI we have tacitly assumed that the resonance near 60 cm^{-1} (Figs. 3 and 5) is due to the motion of silver ions only. On the other hand, our lattice-dynamical calculations based on the antiperovskite structure (in which the silver ions are located at the face centers) indicate that this mode not only involves the silver ions but to some extent also the iodine and sulfur ions. If the double-well model is applied to β-Ag_3SI, the parameters such as the mass, the oscillator frequency and strength and the damping should therefore be regarded as *effective* parameters which are associated with the real normal mode. Nevertheless, the fact that it is possible to describe both the oscillation and the jumps with the double-well model indicates, that this normal mode can, in a certain approximation, be regarded as the attempt mode for jumps of silver ions. The real attempt mode (reaction coordinate for jumps) is a superposition of all the normal modes.

Finally, it should be mentioned that β-Ag_3SI represents a system which could, in principle, be described on the basis of a generalized lattice-dynamical model developed by Merten *et al.*[10–12] In this model the normal modes of the system are coupled to the Debye relaxation via the effective field. The Debye relaxation represents the jumps of ions between different nearby sites of one or more sublattices. It has also been shown that this coupling can lead to order-disorder transitions and could possibly explain the $\beta\rightarrow\gamma$ phase transition of Ag_3SI. The application of this model to Ag_3SI is, however, very cumbersome due to the three silver sublattices and the many parameters involved and is therefore beyond the scope of this paper.

ACKNOWLEDGMENTS

We would like to thank Dr. T. Hibma, Dr. L. Pietronero, Dr. W. R. Schneider, and Dr. H. R. Zeller for helpful discussion and Mr. W. Foditsch for his skilled technical assistance during the measurements.

APPENDIX

Within a memory function ansatz the mobility is given by

$$\mu(\omega)=\left[-i\omega+\gamma+\omega^{*2}\left[\frac{b}{-i\omega}+\frac{1-b}{-i\omega+1/\tau'}\right]\right]^{-1}.$$

Here

$$\tau'=\frac{\Gamma-\gamma}{\omega^{*2}-\Omega_0^2},$$

where

$$\Gamma=\Omega_0^2\frac{\tau_{\rm esc}}{2},$$

$$b=\Omega_0^2/\omega^{*2},$$

and

$$\Omega_0=1/\sqrt{\alpha(0)}.$$

The static polarizability is given by

$$\alpha(0)=2\frac{4\Delta}{k_BT\omega_0^2}u\left[\frac{4\Delta}{k_BT}\right],$$

where

$$u(x)=\frac{\int dy\, e^{-x[(1/4)y^4-(1/2)y^2]}y^2}{\int dy\, e^{-x[(1/4)y^4-(1/2)y^2]}}$$

has been taken from a table. The renormalized frequency ω^* is given by

$$\omega^{*2}=\omega_0^2[3u(x)-1]/2.$$

The escape rate $1/\tau_{\rm esc}$ becomes

$$1/\tau_{\rm esc}=\frac{\omega^*}{2\pi}\left\{\left[1+\left[\frac{\gamma}{2\omega_1}\right]^2\right]^{1/2}-\frac{\gamma}{2\omega_1}\right\}e^{-\Delta/k_BT},$$

where

$$\omega_1=\omega_0\sqrt{2}.$$

[1]B. Reuter and K. Hardel, Anorg. Allg. Chem. 340, 158 (1965); 340, 168 (1965).

[2]B. Reuter and K. Hardel, Ber. Bunsenges. Phys. Chem. 70, 82 (1966).

[3]S. Hoshino, T. Sakuma, and Y. Fujii, J. Phys. Soc. Jpn. 45, 705 (1978).

[4]S. Hoshino, T. Sakuma, and Y. Fujii, J. Phys. Soc. Jpn. 47, 1252 (1979).

[5]E. Perenthaler, H. Schulz, and H. U. Beyeler, Acta Crystallogr. B 37, 1017 (1981).

[6]E. Perenthaler, H. Schulz, and H. U. Beyeler, Solid State Ionics 5, 493 (1981).

[7]E. Perenthaler and H. Schulz, Solid State Ionics 2, 43 (1981).

[8]D. H. Martin and E. Puplett, Infrared Phys. 10, 105 (1969).

[9]P. Brüesch and W. Foditsch, J. Phys. E 12, 872 (1977).

[10]L. Merten and P. R. Andrade, Phys. Status Solidi B 62, 641 (1974).

[11]C. H. Tillmanns, L. Merten, and G. Borstel, in *Proceedings of the International Conference on Lattice Dynamics, Paris, 1977,* edited by M. Balkanski (Flammarion, Paris, 1978), p. 695.

[12]C. H. Tillmanns, L. Merten, Z. Naturforsch. Teil A 33, 808 (1978).

[13]W. R. Schneider and S. Strässler, Z. Phys. B 27, 357 (1977).

[14]S. Chandrasekhar, Rev. Mod. Phys. 15, 1 (1943).

[15]See, for instance, F. Wooten, *Optical Properties of Solids* (Academic, New York, 1972), p. 77.